

A simple empirical method for high-quality electron microprobe analysis of fluorine at trace levels in Fe-bearing minerals and glasses

JEFFREY B. WITTER* AND SCOTT M. KUEHNER

Department of Earth and Space Sciences, University of Washington, Seattle, Washington 98195, U.S.A.

ABSTRACT

We present a new, high-quality electron microprobe method for analyzing F in Fe-bearing minerals and glasses down to trace levels (<1000 ppm F). This method is empirically based and corrects for the problem of overlap of the $FK\alpha$ peak onto the “shoulder” of the $FeL\alpha_1$ peak that arises when using synthetic multi-layered diffraction crystals. It also achieves high precision and accuracy while maintaining low detection limits and a small beam diameter. Analytical conditions for F using the new method and a synthetic W/Si diffraction crystal are: 10 kV accelerating voltage, 180 nA beam current, 8 μm beam diameter, and 400 second total peak count time. An iterative beam exposure method is employed to minimize potential damage to the sample due to beam heating. The method presented here can be used to address problems related to degassing of F at active volcanoes, the reservoirs of F in the mantle, and the partitioning of F between minerals and silicate liquid.

INTRODUCTION

Fluorine is commonly found dissolved in the silicate glass phase of volcanic rocks with concentrations from a few hundred to several thousand parts per million (Dunbar and Hervig 1992a, 1992b; Michael and Schilling 1989; Signorelli et al. 1999b, 2001). It is also the fifth most abundant component of gases liberated from active volcanoes (following H_2O , CO_2 , S-gases, and Cl; Symonds et al. 1994). Fluorine is an important volatile element, found in minor to trace quantities, in common igneous and metamorphic minerals such as amphibole and mica (Deer et al. 1992). Fluorine also may be present in trace amounts in the nominally anhydrous minerals olivine and pyroxene (Hazen et al. 1997; Hoskin 1999). The precise and accurate micro-analysis of F at low levels of detection (tens of parts per million) in minerals and silicate glass is important for determining the systematics of F in volcanic systems and the reservoirs of F in the mantle. For example, high-quality analysis of F on the micrometer scale would be an improvement over bulk analysis of mineral and glass separates to determine partition coefficients between the rims of F-bearing minerals and their coexisting silicate liquids (Métrich 1990). In addition, a comparison of F contents in glass inclusions in phenocrysts and coexisting matrix glasses can assess the extent of F degassing to the atmosphere during volcanic eruptions (Devine et al. 1984). The determination of F in mantle olivine and pyroxene could test the hypothesis that these phases are a significant mantle reservoir for F in addition to H_2O (Bell and Rossman 1992). The development of analytical methods for analyzing F with the electron microprobe (EMP) is useful due to the ubiquity of these instruments worldwide. Our method could also provide an instructive comparison with other correction schemes available in some EMP automation systems (e.g., SAMx XMAS); however, it would be most useful for those laboratories that do not have access to the appropriate software packages.

Analysis of trace levels of F (<1000 ppm) in Fe-bearing

minerals and glasses is not routine in most electron microprobe labs (unlike other volatile elements S and Cl), for a variety of reasons. Conventional TAP diffraction crystals have low count rates for $FK\alpha$ X-rays resulting in high minimum detection limits and large errors based on counting statistics (Potts and Tindle 1989). Utilizing a TAP crystal with a high beam current and/or long count time, to reduce the minimum detection limit of F, can be problematic due to potential sample damage by the electron beam, including volatile migration. Synthetic multi-layered diffraction crystals [W/Si; termed LDE1 ($2d = 60 \text{ \AA}$) by JEOL and PC0 ($2d = 45 \text{ \AA}$) and PC1 ($2d = 60 \text{ \AA}$) by Cameca], which are customized for the diffraction of light element X-rays, provide much higher count rates. However, an overlap of the $FK\alpha$ peak onto the “shoulder” of the $FeL\alpha_1$ peak makes analyzing F in Fe-bearing minerals and glasses difficult when using W/Si (Potts and Tindle 1989).

To overcome these analytical challenges, we developed an electron microprobe method of F analysis using a synthetic multi-layer diffraction crystal that corrects for the presence of Fe using a simple empirical model. We optimized analytical conditions to achieve low detection limits (~35 ppm) at high precision (~5% relative at ~1000 ppm F and ~11% relative at ~400 ppm F) and good spatial resolution (8 μm beam diameter), while minimizing beam damage and/or volatile mobility in sensitive materials such as silicate glass.

OTHER EMP METHODS FOR F ANALYSIS

The literature has many records of various analytical methods to determine F concentration by electron microprobe. We chose not to use any of these previously described methods because detection limits are too high and/or beam diameters are too large for our needs. Several workers have analyzed F in glass inclusions trapped in phenocrysts and matrix glasses in tephra using a TAP crystal and relatively standard microprobe analytical conditions: 15 kV accelerating voltage, 10–25 nA beam current, 1–10 μm beam diameter, and 40–200 second peak count time (Devine et al. 1984; Palais and Sigurdsson 1989; Signorelli et al. 1999a, 1999b, 2001). Minimum detection limits (MDL) of ~300–2000

* E-mail: witt_98103@yahoo.com

ppm F and precisions of 5–25% were reported.

Lowenstern et al. (1994) analyzed F in rhyolitic glass inclusions in quartz crystals using a 30 nA beam current, 20 μm beam diameter, 30 second peak count time, and an LDE1 diffraction crystal. They report a 2σ counting uncertainty of 100 ppm F at a concentration of 3720 ppm F and MDL of 370 ppm F. Repeat analyses on one glass inclusion gave a 2σ variation of ± 440 ppm F. Lowenstern et al. (1994) analyzed the same glass inclusions for F by Secondary Ion Mass Spectrometry (SIMS). On average, F-analyses by EMP are 20% lower than the SIMS analyses, which is greater than the 2σ errors of the two methods based on counting statistics. Based on their Table 3, Lowenstern et al. chose a lower background position near to the Fe $L\alpha_1$ peak. Rhyolitic glasses in their study contain ~ 0.7 wt% FeO (their Table 5). It is possible that the F analyses by EMP are underestimates as a result of the low background position placed near a small but significant Fe $L\alpha_1$ peak.

Michael and Schilling (1989) analyzed F in submarine MORB glasses using a TAP crystal, 8 kV accelerating voltage, 100 nA, and a raster area of $50 \times 30 \mu\text{m}$ to minimize damage to the glass. Counts were collected for 500 seconds on the peak position and 250 seconds each on two symmetrically offset background positions. They reported precision (2σ) of 30 ppm F based on counting statistics and reproducibility of ~ 40 ppm F at a concentration of 250 ppm F. This method reproduces the F concentration within 2σ in three out of four standards analyzed by the ion selective electrode method (Schilling et al. 1980).

Thordarson et al. (1996) analyzed F in basaltic glass inclusions in olivine and co-existing matrix glasses using a PCO diffraction crystal, 15 kV accelerating voltage, 80 nA beam current, 10 μm beam diameter, and 400 second peak count time. Thordarson et al. (1996) utilized the CSIRO-trace routine of Robinson and Graham (1992), an iterative method that blanks the beam every 10 seconds. Precision (2σ) of 90 ppm F based on counting statistics was reported for F abundances of ~ 500 ppm. Although they made no mention of addressing the problem of Fe peak overlap in their EMP method, their method reproduced the F concentrations determined by Michael and Schilling (1989) using a TAP crystal on the same standard material.

Métrich et al. (2001) analyzed F in Fe-bearing basalt glasses using analytical conditions of 10 kV accelerating voltage, 15 μm beam diameter, and 40–80 nA beam current. They reduced their analytical error by counting F on two TAP crystals simultaneously. They report an MDL of 210 ppm F with 11% relative error for 900 ppm F with a 400 second total (peak and background) count time (Nicole Métrich, pers. comm. 2002).

Donovan et al. (1993) developed an iterative model for correcting spectral interferences applicable to the analysis of F in Fe-bearing minerals and glasses that is incorporated into some commercial EMP automation packages (e.g., SAMx XMAS). We attempted to utilize the method of Donovan et al. (1993) in our analysis of trace levels of F, but abandoned it for the following reason. The method of Donovan et al. requires the determination of the intensity of the overlapping element at the peak location of the element of interest in a standard free of the element of interest. This intensity is then used to estimate the amount of overlap with the characteristic X-ray line of interest in the unknown. We used hematite (Fe $_2$ O $_3$, 69.9 wt% Fe) as our interference standard

for Fe and determined the intensity of X-rays derived from Fe at the FK α peak position. The high concentration of Fe in hematite produces a large number of counts at the FK α peak position. Although the high count rate for Fe results in a small statistical error, the randomness in terms of total counts measured is overwhelming when compared to the randomness in the small number of characteristic X-ray counts derived from the excitation of F atoms at trace levels. We found that when using the method of Donovan et al. to analyze samples with less than 1000 ppm F, the combination of the relatively large variability of X-ray counts in the interference standard and the small measured F signal results in a large uncertainty in the final F concentration. In the present study, we do not attempt a direct comparison between results of analyses of trace levels of F using our method and the method of Donovan et al. or others; however, such a comparison in the future would be instructive.

Todd (1996) outlined an electron microprobe method for analyzing F in Fe-bearing minerals using a PCO diffraction crystal. He reported that a linear relationship exists between wt% FeO and apparent wt% F in F-free standards such as olivines, pyroxenes, and oxides: apparent wt% F = $0.0167 + 0.00619 \times \text{FeO wt\%}$. In this method, the F correction equation is applied following the matrix correction algorithm.

Although our method builds on the work of Todd (1996) and Thordarson et al. (1996), it differs in that we have created an F-correction equation that is an internal part of the analytical routine and is applied prior to the matrix correction algorithm. Our method solves both problems of beam heating and peak overlaps and can be implemented on any microprobe.

ANALYTICAL METHOD

The F analysis method presented here was developed on a 4-spectrometer JEOL 733 Superprobe (140 mm Rowland circle radius, 40° take-off angle) with Geller automation at the University of Washington. The method consists of two parts. First, we describe an improved iterative routine that attains high precision and low detection limits while minimizing beam damage and volatile mobility. Second, we present an empirical correction scheme for Fe $L\alpha_1$ peak interference on the FK α peak.

Analytical conditions for F analysis are as follows: LDE1 diffraction crystal (Ovonxy OV-060A), 10 kV accelerating voltage, 180 nA beam current, 8 μm beam diameter, and 400 second total peak count time. A high beam current of 180 nA is utilized to produce high count rates. The beam diameter was set at 5 μm on the JEOL hardware, which resulted in a measured beam diameter of $\sim 8 \mu\text{m}$ at these analytical conditions (Goldstein et al. 1981). A beam diameter of 8 μm is a good compromise to reduce sample heating [by a factor of ~ 5 compared to $\sim 1 \mu\text{m}$ diameter beam, according to the equation of Castaing (1951)], while still providing good spatial resolution for assessing F-zonation in minerals or for the analysis of small ($>10 \mu\text{m}$) glass inclusions contained in phenocrysts. Compared to higher accelerating voltages, the reasons for running analyses at an accelerating voltage of 10 kV are: (1) improved efficiency of F X-ray production; (2) shallower analytical volume; and (3) smaller ZAF correction due to shorter path length. Detector PHA settings for F were differential mode, bias of 1830, baseline of 0.5v, window of 3v, and gain of 2. We do not recommend that these extreme analytical conditions be used to analyze all the other elements in a sample (particularly major elements) due to high dead times, pulse height depression, etc. In our laboratory, however, we have found success at analyzing trace S and Cl simultaneously with F at the above analytical conditions. For samples of unknown composition, we normally analyze major and minor elements in a separate analytical session, under more routine analytical conditions, prior to the analysis of S, Cl, and F.

Volatile loss during the analysis, due to the very high beam current, is minimized through the use of both a large beam spot (8 μm) and an iterative scheme that blanks the electron beam for 10 seconds after each 10 second counting interval, allowing the sample to cool. A short "macro" program written for the Geller automation system controls the periodic blanking of the electron beam (see Appendix A). The total number of F peak counts is the summation of forty

successive iterations for a total F peak counting time of 400 seconds. Background counts are collected in a similar manner for a total background counting time of 400 seconds. We conducted a test of volatile mobility under the electron beam in basaltic glass standards and found that X-ray count rates for F remain stable during the entire period of analysis. Our method is a modified version of the routine originally developed by T. Thordarson at the University of Hawaii (see Thordarson et al. 1996). Note that a rastered beam should never be used as a means to minimize beam heating, nor for any quantitative analysis, as not all portions of the rastered area experience the same dwell time.

The ideal F-peak position on the LDE1 diffraction crystal ($2d = 60 \text{ \AA}$) used in the University of Washington electron microprobe is at an L-value of 83.60 mm ($0.29857 \sin\theta$ units or $\lambda = 17.914 \text{ \AA}$). We chose only one background position, at an L-value of 85.60 mm ($0.30571 \sin\theta$ units or $\lambda = 18.343 \text{ \AA}$), to avoid the nearby $\text{AlK}\alpha$ II peaks and $\text{MgK}\alpha$ II (Fig. 1). Fluorine was calibrated on an Fe-free synthetic F-phlogopite standard (9.02 wt% F) prior to each analytical session.

The major challenge for accurate analysis of F is correcting the spectral interference between the $\text{FK}\alpha$ peak and the $\text{FeL}\alpha_1$ line (Fig. 1). To overcome this problem, we first measured the number of counts at the $\text{FK}\alpha$ peak position on a variety of F-free standards containing 0–30 wt% Fe (Fig. 2). Background counts were also collected on one side (the high side) of the $\text{FK}\alpha$ peak on each F-free standard. Background counts were not collected on the low side of the $\text{FK}\alpha$ peak position due to interference from the $\text{FeL}\alpha_1$ peak. Our analysis of the $\text{FK}\alpha$ peak and background positions for nine F-free standards shows that the slope of the “shoulder” of the $\text{FeL}\alpha_1$ peak increases with increasing Fe-concentration (Fig. 2). We posit that this systematic increase in slope is wholly due to the increasing Fe-content in the F-free standards and the increasing size of the $\text{FeL}\alpha_1$ peak. Slight changes in the slope and intensity of the “Bremsstrahlung” due to minor differences in the mean atomic numbers for the different F-free standards are considered to be negligible and, indeed, we conducted wavelength scans of a variety of F- and Fe-free silicate mineral and glass standards, and found the slope of the “Bremsstrahlung” to be very similar between standards over the spectrometer range of interest (L-value = 81–86 mm, $0.2893 - 0.3071 \sin\theta$ units, or $\lambda = 17.357 - 18.429 \text{ \AA}$).

We calculated a ratio, called C_{Factor} , to represent the fractional amount that the X-ray counts at the $\text{FK}\alpha$ peak position exceed X-ray counts at the F background position in these F-free standards of varying Fe-content:

$$C_{\text{Factor}} = N_{\text{peak}}^{\text{F}} / N_{\text{bkg}}^{\text{F}} \quad (1)$$

where $N_{\text{peak}}^{\text{F}}$ = number of counts at the F peak position for the F-free standards and $N_{\text{bkg}}^{\text{F}}$ = number of counts at the F background position. For these F-free standards, the counts collected at the $\text{FK}\alpha$ peak position are the sum of the $\text{FeL}\alpha_1$ “shoulder” and the “Bremsstrahlung” radiation (Fig. 3). Our measurements of $N_{\text{peak}}^{\text{F}}$ and $N_{\text{bkg}}^{\text{F}}$ in the F-free standards show that, within analytical error, the C_{Factor} varies linearly with Fe content (Fig. 4). For solids that contain 0 wt% Fe, the $C_{\text{Factor}} \sim 1.1$, due to the non-zero slope of the background “Bremsstrahlung” radiation. Based upon

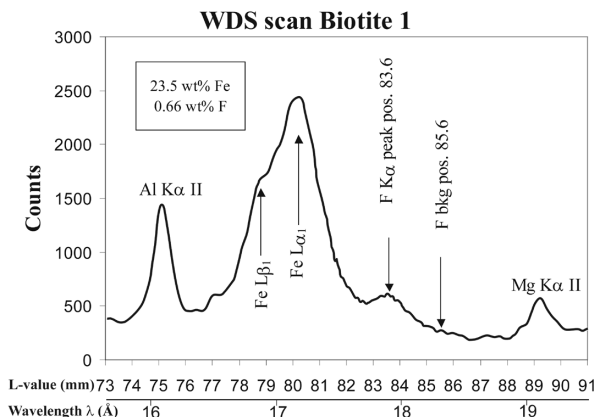


FIGURE 1. Wavelength scan of the LDE1 diffraction crystal in the region of the $\text{FK}\alpha$ peak for the mineral standard Biotite 1 (which contains 23.5 wt% Fe and 6600 ppm F). Peaks for $\text{AlK}\alpha$ II, $\text{FeL}\beta_1$, $\text{FeL}\alpha_1$, $\text{FK}\alpha$, and $\text{MgK}\alpha$ II lines are shown. The chosen F background position is also shown. Note the position of the $\text{FK}\alpha$ peak on the “shoulder” of the $\text{FeL}\alpha_1$ peak.

our determinations of the C_{Factor} for a variety of F-free, Fe-bearing standards, we derived a linear least-squares equation for the best-fit line that relates C_{Factor} to Fe-content (Fig. 4):

$$C_{\text{Factor}} = 0.0085 \times \text{Fe wt\%} + 1.1108 \quad (2)$$

It must be noted that this equation for the best-fit line may be slightly different when derived from data obtained from other F-free standards, on different EMP platforms, or using different W/Si diffraction crystals. To ensure the highest accuracy, we recommend that Equation 2 be derived independently by each laboratory.

In the F analysis method described here, the ratio, C_{Factor} , is used to correct for the $\text{FeL}\alpha_1$ “shoulder” overlying the F peak position as well as the non-zero slope of the “Bremsstrahlung.” If the Fe-content of a sample to be analyzed is known, the number of counts derived from the “Bremsstrahlung” and the Fe “shoulder” at the F peak position ($N_{\text{peak}}^{\text{F}}$, Fig. 3) can be calculated by simply multiplying the number of counts measured at the background position ($N_{\text{bkg}}^{\text{F}}$) by the appropriate C_{Factor} calculated from the known Fe-content (Eq. 2):

$$N_{\text{peak}}^{\text{F}} = N_{\text{bkg}}^{\text{F}} \cdot C_{\text{Factor}} = N_{\text{calc}}^{\text{F}} \quad (3)$$

The calculated number of counts derived from the “Bremsstrahlung” and the Fe “shoulder” at the F peak position is subsequently referred to as $N_{\text{calc}}^{\text{F}}$.

Accuracy of the F analysis technique was tested using internal mineral standards Biotite1, Biotite23a, Biotite27, Mason Biotite, Glaucofane, and Muscovite-M. These mineral standards have F-contents ranging from 300 to 6600 ppm (Table 1). The technique was tested further on NIST glass standards SRM610 and SRM620; NMNH glass standard A99; and glass standards KE12, KE3, CFA47 (provided by N. Métrich). The glass standards have F contents ranging from 0 to 4700 ppm (Table 1).

For the analysis of the mineral and glass standards that contain both F and Fe, the number of counts at the F peak ($N_{\text{peak}}^{\text{total}}$) and background ($N_{\text{bkg}}^{\text{F}}$) positions were measured (Fig. 3). The number of counts due to the “Bremsstrahlung” and the Fe “shoulder” at the F peak position were calculated ($N_{\text{calc}}^{\text{F}}$) using Equations 2 and 3 and the known Fe content of the standard under analysis. The number of counts

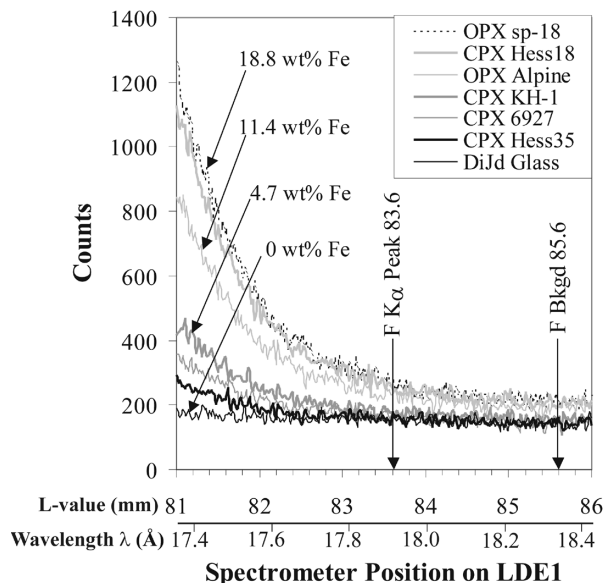


FIGURE 2. Wavelength scans of the LDE1 diffraction crystal in the region of the $\text{FK}\alpha$ peak for a variety of F-free standards of varying Fe content. Wavelength scans are superimposed to show the increase in slope of the “shoulder” of the $\text{FeL}\alpha_1$ peak with increasing Fe content. The $\text{FK}\alpha$ peak position and F background position are shown. The $\text{FeL}\alpha_1$ peak position is off the left side of the chart at an L-value of 80.2 mm. For clarity, not all Fe concentrations are indicated. These are: CPX Hess 35, 2.22 wt% Fe; CPX 6927, 2.95 wt% Fe; and CPX Hess 18, 18.65 wt% Fe. Curve for Olivine YS-15 (29.77 wt% Fe) and quartz (0 wt% Fe) not shown.

TABLE 1. Accepted Fe and F contents of mineral and glass standards analyzed in this study

Glass Standard	Fe (wt%)	F (ppm)	2σ	Mineral Standard*	Fe (wt.%)	F (ppm)	2σ†
A99 ^a	10.34	765	±144	Biotite 1 ^h	23.46	6600	n.r.
KE12 ^b	6.50	4000	±240	Biotite 23a ⁱ	20.93	3600	n.r.
KE12 ^c	6.50	4338	±1096	Biotite 27 ⁱ	16.91	5100	n.r.
KE12 ^d	6.50	4400	n.r.	Mason Biotite ^k	14.52	2100	n.r.
KE3 ^e	5.68	4700	n.r.	Glaucofane ^l	9.61	300	n.r.
CFA47 ^b	2.06	2000	±120	Muscovite-M ^m	3.96	1000	n.r.
CFA47 ^f	2.06	2500	±1200				
NIST SRM 610 ^g	0.05	295	±32				
NIST SRM 620	0.03	0	n.r.				

Notes: n.r. = not reported; 2σ = error on the F-analysis; EMP = electron microprobe; SIMS = secondary ion mass spectrometry; ISE = ion selective electrode. a = EMP analyses reported in Thordarson et al. (1996); b = ISE analyses reported in Mosbah et al. (1991); c = EMP analyses reported in Palais and Sigurdsson (1989); d = accepted value reported in Palais and Sigurdsson (1989); e = accepted value reported in Mosbah et al. (1991); f = EMP analyses reported in Signorelli et al. (1999b); g = SIMS analyses reported in Hoskin (1999); h = Wet chemistry, I. Carmichael, UC Berkeley; i = Geological Survey of Canada; j = Rimsaite (1964); k = Mason (1962); l = Borg (1967); m = Evans (1965).

* = All analyses of F in mineral standards conducted by classical wet chemistry methods.

† = An error of + 1000 ppm F is assumed for the wet chemical method.

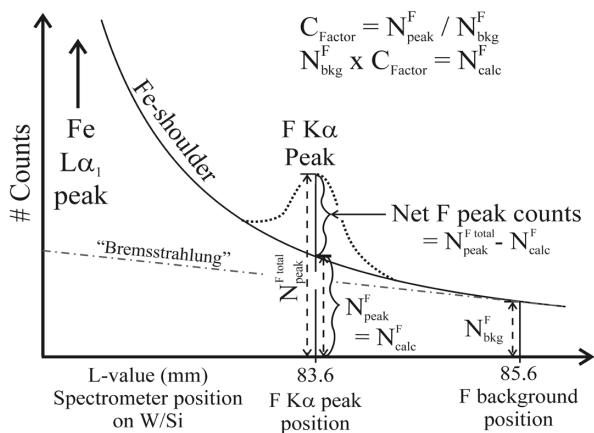


FIGURE 3. A schematic diagram showing a wavelength scan of the LDE1 diffraction crystal in the region of $FK\alpha$ peak illustrating our method of determining the contribution of X-ray counts at the F peak position due to the $FeL\alpha_1$ peak. The “shoulder” of the $FeL\alpha_1$ peak is shown as a solid sloping line. The $FK\alpha$ peak is shown as a dotted line. The inclined “Bremsstrahlung” radiation is shown by the grey dash-dot line. The number of counts at the F background position (N_{bkg}^F) and the number of counts at the $FK\alpha$ peak position (N_{peak}^F) due to the $FeL\alpha_1$ “shoulder” are measured on F-free standards. The value of the correction factor (C_{Factor}) is calculated from the ratio of $N_{peak}^F:N_{bkg}^F$. See text for further explanation.

obtained at the $FK\alpha$ peak position that are derived only from the excitation of F atoms were calculated from the difference between the total counts at the F peak position ($N_{peak}^{F_{total}}$) and the calculated number of counts (N_{calc}^F) due to the “Bremsstrahlung” and the Fe “shoulder” at the F peak position (see Fig. 3). The resulting net number of F counts was then inserted into a table with known major-element concentrations of the glass and mineral standards and the matrix corrections calculated via the method of Armstrong (1984).

For analyzing F in Fe-bearing unknowns (e.g., glass inclusions, matrix glass, minerals), the net number of F counts can be inserted into a table with major-element data for the unknown that were collected previously (under routine analytical conditions). The fluorine data are then processed with the major element data and the appropriate matrix corrections are applied.

As an alternative, if one chooses to determine all elements, including F, simultaneously (under the same analytical conditions) then C_{Factor} can be determined during analysis by simply estimating the Fe wt% via the relationship:

$$C_{unk}^{Fe} = C_{std}^{Fe} \frac{I_{unk}^{Fe}}{I_{std}^{Fe}} \quad (4)$$

where C_{unk}^{Fe} = the concentration of Fe in the unknown, C_{std}^{Fe} = the concentration of Fe in the standard, I_{unk}^{Fe} = intensity of Fe in the unknown, and I_{std}^{Fe} = intensity of Fe

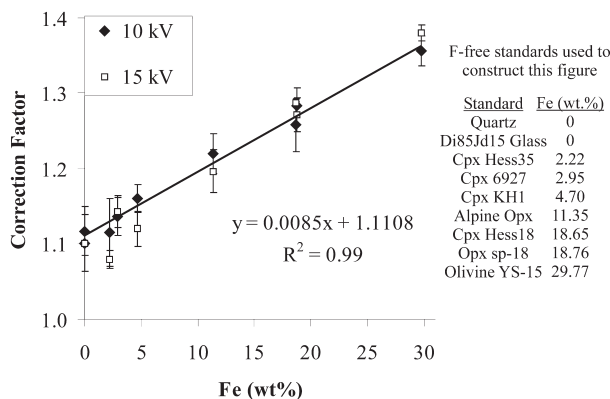


FIGURE 4. Plot of Fe-content in F-free standards vs. correction factor, C_{Factor} . The correction factor was calculated using nine F-free standards with varying Fe content (Fig. 2) using the following formula: $C_{Factor} = N_{peak}^F / N_{bkg}^F$, where N_{peak}^F = number of counts at the $FK\alpha$ peak position and N_{bkg}^F = number of counts at the F background position (see Fig. 3). For each standard we collected counts at 10 kV (filled diamonds) on the peak and background positions five times for 30 seconds each time and averaged the results. This process was repeated for each standard at 15 kV (open squares) for comparison. Error bars are 2σ standard deviations. Agreement between analyses done at 10 kV and 15 kV are within error. The solid line represents the linear least squares regression for the 10 kV analyses. The equation for this line and R^2 statistic are shown.

in the standard. The net F intensity can then be calculated and matrix corrections applied to all elements simultaneously.

RESULTS

We analyzed several mineral and glass standards with known F contents that range from zero to several thousand parts per million F. As a test of the quality of our Fe-correction scheme, we analyzed F in mineral standards that contain both Fe and F with TAP and LDE1 diffraction crystals simultaneously (Fig. 5; Table 2). Although the analyses with TAP are less precise than LDE1, we would expect the results using the two different diffraction crystals to overlap if our correction scheme is accurate. Agreement between the results obtained with the two diffraction crystals is very good. As there are no spectral interferences when analyzing F with the TAP crystal, this agreement suggests that the correction scheme presented here adequately corrects for overlap of the $FK\alpha$ peak on the “shoulder” of the $FeL\alpha_1$ peak

TABLE 2. Comparison of EMP analysis of fluorine using different diffraction crystals for mineral standards containing both F and Fe

Sample	LDE1			TAP			Accepted F (ppm)
	F (ppm)	2σ	MDL	F (ppm)	2σ	MDL	
Glaucofane	399	44	37	107	87	82	300
Muscovite-M	2076	42	35	1801	126	82	1000
Mason Biotite	2520	48	39	2424	121	92	2100
Biotite 23a	3804	53	42	3868	155	96	3600
Biotite 27	6150	62	44	6005	180	95	5100
Biotite 1	6602	59	45	n/a	n/a	n/a	6600

Notes: Iron contents of the analyzed mineral standards are listed in Table 1. EMP analysis by TAP and LDE1 conducted simultaneously under identical analytical conditions. 2σ = error based on counting statistics; MDL = minimum detection limit; n/a = not analyzed.

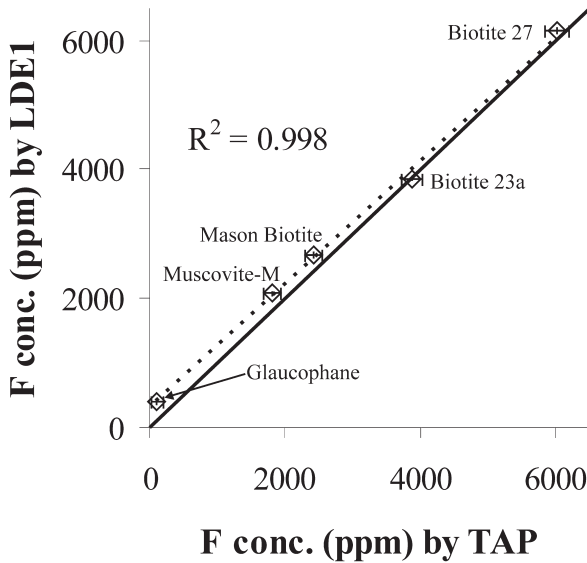


FIGURE 5. Comparison of EMP analysis of fluorine in F- and Fe-bearing mineral standards using different diffraction crystals. EMP analysis of the same spot by TAP and LDE1 conducted simultaneously under identical analytical conditions (described in the text). Each data point represents one analysis. Heavy solid line is the 1:1 line. Two-sigma error based on counting statistics is shown. Light dashed line is the linear least squares regression through the data with R² statistic shown. The data used to construct this figure are listed in Table 2. The mineral standard Biotite 1 was not analyzed with TAP.

and the sloping “Bremsstrahlung.”

A comparison between the F content determined in mineral and glass standards using the LDE1 diffraction crystal and the accepted F content is shown in Figure 6 and Tables 2 and 3. Agreement is quite good between accepted and measured values, especially since the composition of the majority of the mineral standards were determined by wet chemistry which, because this is a bulk analytical method, will average any chemical inhomogeneities present in the sample. We estimate the analytical errors in the wet chemical analysis to be ±0.1 wt% F (Bernard Evans, personal communication 2002).

Average analytical errors (2σ) of the F analyses based on counting statistics are 13% at 300 ppm F and 1.8% at 2500 ppm F as determined from the following equations:

$$\% \sigma = \frac{\sqrt{N_{\text{peak}}^{\text{F total}} + N_{\text{calc}}^{\text{F}}}}{N_{\text{peak}}^{\text{F total}} - N_{\text{calc}}^{\text{F}}} \quad \% \text{ relative error } (2\sigma) = 2\sqrt{\% \sigma_{\text{unk}}^2 + \% \sigma_{\text{std}}^2} \quad (5)$$

Minimum detection limits are calculated using the method of Reed (1975):

TABLE 3. Analyses of F in glass standards using LDE1 diffraction crystal

Standard	F conc.	2σVar.	2σ Err	MDL	n
KE3	5130	138	51	37	2
KE12	4513	88	50	36	2
CFA47	2483	32	45	33	2
A99	976	8	45	36	2
NIST SRM 610	336	24	42	31	3
NIST SRM 620	0	0	n/a	30	4

Notes: All analyses made with the LDE1 synthetic multi-layer diffraction crystal. All results reported as ppm.

n = number of analyses; conc. = concentration; 2σ Var. = two-sigma variation in the multiple analyses of a single standard; 2σ Err = two-sigma error based on counting statistics; MDL = minimum detection limit.

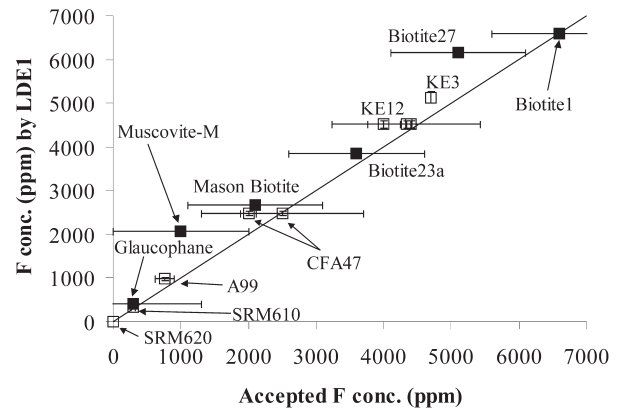


FIGURE 6. Comparison of accepted and measured F concentration in mineral (filled squares) and glass standards (open squares). Fluorine measured by EMP using an LDE1 diffraction crystal and analytical conditions described in the text. Heavy solid line is the 1:1 line. Two-sigma errors based on counting statistics for the EMP analysis are the same size or smaller than the symbols for mineral analyses and are shown for glass standard analyses. Analytical errors on the accepted values of the mineral standards are estimated to be ±1000 ppm F. Error bars on the accepted values of the glass standards show the two-sigma error based on counting statistics or the two-sigma variation on multiple analyses on a single standard, whichever is greater. The accepted value of the glass standard A-99 is dubious because it is based on electron microprobe analyses using a multi-layer diffraction crystal. Whether or not a correction for spectral interference between F and Fe was undertaken to determine the accepted value is unknown. The analytical method used to determine the accepted value of glass standard KE3 is also unknown, as are the errors associated with that analysis.

$$\text{Minimum Detection Limit} = \frac{4C_b}{\sqrt{N_{\text{peak}}^{\text{F total}} + N_{\text{calc}}^{\text{F}}}} \quad (6)$$

$$C_b = C_{\text{std}} \left(\frac{I_{\text{bkg}}}{I_{\text{std}}} \right)$$

where C_b = the “apparent concentration” of the background, C_{std} = the

concentration of F in the standard, I_{std} = the total F peak intensity of the standard, and I_{bkg} = intensity of the background in the unknown. We obtain a minimum detection limit of 35 ppm F using this relationship.

DISCUSSION

Due to the high beam currents employed in the analyses (180 nA), we might suspect Na migration to occur in silicate glasses despite utilization of an iterative beam blanking method to minimize this effect. Appreciable loss of Na during the analysis could affect the concentration of F in unpredictable ways. For example, a decreasing Na content due to Na migration in the region under the electron beam might result in a decreasing absorption of $FK\alpha$ X-rays by Na and, therefore, an increasing F count rate over the course of the analysis. Also, if significant Na loss occurs (i.e., several wt%) and it is not taken into account, a ZAF correction that utilizes the pre-analysis Na content would be inaccurate. Both of these effects would result in an anomalously high apparent concentration of F. We performed several tests to assess the effect of Na migration on our analyses of silicate glasses. Note that the effect of Na migration on the mineral standards used in this study was insignificant due to their low Na contents ($\text{Na}_2\text{O} < 0.3$ wt%). The Na-migration effect was not tested on the Glaucofane mineral standard ($\text{Na}_2\text{O} = 6.55$ wt%).

For all of the glass standards, we found count rates for Na dropped dramatically during the course of the analysis. In F- and Fe-bearing alkaline glasses [with $(\text{Na} + \text{K})/\text{Al} > 1$; e.g., SRM 610 (13.8 wt% Na_2O), KE12 (7.3 wt% Na_2O), and KE3 (6.8 wt% Na_2O)], Na counts fell exponentially in the first few iterations of the analysis and remained low for the remainder of the analysis. Interestingly, F counts increased linearly throughout the entire analysis by 6–8% relative. The observation that Na loss is exponential while F counts increase linearly may suggest that electron beam-induced changes to the matrix may be quite complex and may involve additional effects such as K loss and/or Si and Al “grow-in” (Morgan and London 1996). It must be noted that the alkaline glass standards KE12 and KE3 represent extreme compositions not commonly found in nature, and the glass standard SRM 610, although chemically well characterized, represents a composition that is virtually non-geological. In contrast to the alkaline glasses, analysis of F- and Fe-bearing calc-alkaline glasses [$(\text{Na} + \text{K})/\text{Al} < 1$; e.g., A99], showed that Na counts decreased in an approximately linear fashion and F count rates remained stable during the course of the analysis.

To assess the effect of an inaccurate ZAF correction due to possibly significant Na loss, we analyzed Na simultaneously with F on the same glass standards mentioned above using the high beam current. We determined the time-averaged Na content and performed the ZAF correction using this measured average Na concentration. Results of these tests are inconclusive because they do not show a consistent trend. We are suspicious that inhomogeneity of fluorine in the glass standards may set a limitation on our ability to evaluate accurately the effect that Na migration may have on the ZAF correction. Overall, we conclude that users should use caution when analyzing F in highly alkaline glasses, and pay special attention to changes in the matrix caused by the use of a high beam current and their possible effects on the measured F concentration.

ACKNOWLEDGMENTS

We thank Nicole Métrich for generously supplying the glass standards KE3, KE12, and CFA47 used in this study. We are also grateful to Bernard Evans for constructive comments on a preliminary version of this work. Thorough reviews by John Fournelle and George Morgan greatly improved this manuscript. This investigation was financially supported by NSF grant no. EAR-9980566 to V. Kress and C. Newhall and a NASA ESS Graduate Fellowship to JBW.

REFERENCES CITED

- Armstrong, J.T. (1984) Quantitative analysis of silicate and oxide minerals: A re-evaluation of ZAF corrections and proposal for new Bence-Albee coefficients. In A.D. Romig Jr. and J.I. Goldstein, Eds., *Microbeam Analysis*, p. 208–212. San Francisco Press, California.
- Bell, D.R. and Rossman, G.R. (1992) Water in Earth's Mantle: The role of nominally anhydrous minerals. *Science*, 255, 1391–1397.
- Castaing, R. (1951) Application des sondes électroniques à une méthode d'analyse ponctuelle chimique et cristallographique. University of Paris.
- Deer, W.A., Howie, R.A., and Zussman, J. (1992) *An Introduction to the Rock-Forming Minerals*. 696 p. Longman Scientific & Technical, Essex, England.
- Devine, J.D., Sigurdsson, H., Davis, A.N., and Self, S. (1984) Estimates of sulfur and chlorine yield to the atmosphere from volcanic eruptions and potential climatic effects. *Journal of Geophysical Research*, 89, 6309–6325.
- Donovan, J.J., Snyder, D.A., and Rivers, M.L. (1993) An improved interference correction for trace element analysis. *Microbeam Analysis*, 2, 23–28.
- Dunbar, N.W. and Hervig, R.L. (1992a) Petrogenesis and volatile stratigraphy of the Bishop Tuff; evidence from melt inclusion analysis. *Journal of Geophysical Research*, B, Solid Earth and Planets, 97(11), ages 15, 129–15, 150.
- (1992b) Volatile and trace element composition of melt inclusions from the lower Bandelier Tuff; implications for magma chamber processes and eruptive style. *Journal of Geophysical Research*, B, Solid Earth and Planets, 97(11), 15, 151–15, 170.
- Goldstein, J.I., Newburg, D.E., Echlin, P., Joy, D.C., Fiori, C., and Lifshin, E. (1981) *Scanning Electron Microscopy and X-ray Microanalysis*. Plenum, New York.
- Hazen, R.M., Yang, H., Prewitt, C.T., and Gasparik, T. (1997) Crystal chemistry of superfluorine phase B ($\text{Mg}_{10}\text{Si}_3\text{O}_{14}\text{F}_2$): Implications for the role of fluorine in the mantle. *American Mineralogist*, 82, 647–650.
- Hoskin, P.W.O. (1999) SIMS Determination of mg g^{-1} level fluorine in geological samples and its concentration in NIST SRM 610. *Geostandards Newsletter*, 23(1), 69–76.
- Lowenstern, J.B., Bacon, C.R., Calk, L.C., Hervig, R.L., and Aines, R.D. (1994) Major-element, trace-element, and volatile concentrations in silicate melt inclusions from the tuff of Pine Grove, Wah Wah Mountains, Utah. U.S. Geological Survey, Open-file Report, 94–242, 1–20.
- Métrich, N. (1990) Chlorine and fluorine in tholeiitic and alkaline lavas of Etna (Sicily). *Journal of Volcanology and Geothermal Research*, 40, 133–148.
- Métrich, N., Bertagnini, A., Landi, P., and Rosi, M. (2001) Crystallization driven by decompression and water loss at Stromboli volcano (Aeolian Islands, Italy). *Journal of Petrology*, 42(8), 1471–1490.
- Michael, P.J. and Schilling, J.-G. (1989) Chlorine in mid-ocean ridge magmas: Evidence for assimilation of seawater-influenced components. *Geochimica et Cosmochimica Acta*, 53, 3131–3143.
- Morgan, G.B. and London, D. (1996) Optimizing the electron microprobe analysis of hydrous alkali aluminosilicate glasses. *American Mineralogist*, 81, 1176–1185.
- Palais, J.M. and Sigurdsson, H. (1989) Petrologic evidence of volatile emissions from major historic and pre-historic volcanic eruptions. In A. Berger, R.E. Dickinson, and J.W. Kidson, Eds., *Understanding Climate Change*, Geophysical Monograph 52, 7, p. 31–53. IUGG and AGU, Washington, D.C.
- Potts, P.J. and Tindle, A.G. (1989) Analytical characteristics of a multilayer dispersion element ($2d = 60 \text{ \AA}$) in the determination of fluorine in minerals by electron microprobe. *Mineralogical Magazine*, 53, 357–362.
- Reed, S.J.B. (1975) Principles of X-ray generation and quantitative analyses with the electron microprobe. In C.A. Anderson, Ed., *Microprobe Analysis*, p. 53–81. Wiley, New York.
- Robinson, B.W. and Graham, J. (1992) Advances in electron microprobe trace-element analysis. *Journal of Computer-Assisted Microscopy*, 4, 263–265.
- Schilling, J.-G., Bergeron, M.B., and Evans, R. (1980) Halogens in the mantle beneath the North Atlantic. *Philosophical Transactions of the Royal Society of London, Series A*, 297(1431), 147–178.
- Signorelli, S., Vaggelli, G., Francalanci, L., and Rosi, M. (1999a) Origin of magmas feeding the Plinian phase of the Campanian Ignimbrite eruption, Phlegrean Fields (Italy): constraints based on matrix-glass and glass-inclusion compositions. *Journal of Volcanology and Geothermal Research*, 91, 199–220.
- Signorelli, S., Vaggelli, G., and Romano, C. (1999b) Pre-eruptive volatile (H_2O , F, Cl, and S) contents of phonolitic magmas feeding the 3550-year old Avellino eruption from Vesuvius, southern Italy. *Journal of Volcanology and Geothermal Research*, 93, 237–256.
- Signorelli, S., Vaggelli, G., Romano, C., and Carroll, M.R. (2001) Volatile element zonation in Campanian ignimbrite magmas (Phlegrean Fields, Italy): evidence from the study of glass inclusions and matrix glasses. *Contributions*

- to Mineralogy and Petrology, 140, 543–553.
- Symonds, R.B., Rose, W.I., Bluth, G.J.S., and Gerlach, T.M. (1994) Volcanic-gas studies: methods, results, and applications. In M.R. Carroll and J.R. Holloway, Eds., Volatiles in Magmas, p. 1–66. Reviews in Mineralogy, Mineralogical Society of America, Washington, D.C.
- Thordarson, T., Self, S., Oskarsson, N., and Hulsebosch, T. (1996) Sulfur, chlorine, and fluorine degassing and atmospheric loading by the 1783–1784 AD Laki (Skaftar Fires) eruption in Iceland. Bulletin of Volcanology, 58(2–3), 205–225.
- Todd, C.S. (1996) Fluorine analysis by electron microprobe: correction for iron interference. Abstract, Annual Meeting, p. A-212. GSA, Boulder, Colorado.

MANUSCRIPT RECEIVED JANUARY 2, 2003

MANUSCRIPT ACCEPTED AUGUST 5, 2003

MANUSCRIPT HANDLED BY EDWARD GHENT

APPENDIX

Below is a portion of the computer program (macro) used on the University of Washington JEOL 733 Superprobe with Geller automation to analyze for fluorine in Fe-bearing minerals and glasses. Analytical conditions used in this study are: 10 kV accelerating voltage, 180 nA beam current, 8 μm beam diameter and a W/Si (LDE1) diffraction crystal for F on spectrometer number 2.

Notes on the syntax of the macro:

- 1) A single quote (') preceding a sentence or phrase in italics denotes a comment line
- 2) The pound sign (#) denotes a variable

`Volatile Macro

`Background correction factor for F

`Enter wt% Fe in unknown here

#Fewtpct = 6.54

`Enter correction factor equation here

*#Cfactor = 0.0085 * #Fewtpct + 1.1108*

`Initialize important variables

#Fpeak = 0; `peak = counts at peak position

#Fbkgdh = 0; `bkgdh = counts at high background position

#Fbkgd1 = 0; `bkgd1 = counts at high background position

collected a second time

#nAtot = 0; `nAtot = sum of beam currents

`Start loop here

#loop = 0; `loop = counter

1

#loop = #loop + 1

#nA BEAM; `command to measure beam current and put the value in variable #nA

`Put spectrometer #2 on the peak position for F

get element F

`Count 10 seconds on peak for F (spec#2)

count 2 10

blank; `insert Faraday cup to blank the electron beam

`Put number of peak counts from spectrometer #2 into appropriate variable

#Fpk = counts 2

`Sum the peak counts

#Fpeak = #Fpeak + #Fpk

`Move spectrometer #2 to background high side

spec 2 by 2

`Count on background high side for 5 seconds for F on spec#2

count 2 5

blank; `insert Faraday cup to blank the electron beam

`Put number of background counts on high side from spec#2 into appropriate variable

#Fbkh counts 2

`Sum the background counts on the high side

#Fbkgdh = #Fbkgdh + #Fbkh

`Leave spectrometer #2 where it is on the high side

`Count on background high side again for 5 seconds for F

count 2 5

blank; `insert Faraday cup to blank the electron beam

`Put number of background counts collected this time into appropriate variable

#Fbkl counts 2

`Sum the background counts collected this time

#Fbkgd1 = #Fbkgd1 + #Fbkl

`Sum the beam current

#nAtot = #nAtot + #nA

`Check to see if 40 iterations have been done yet

if #loop = 40 goto 2

goto 1

2

`Combine total number of counts collected on background high side and increase the total number of measured background counts for fluorine by multiplying by the correction factor #Cfactor.

*#Fbkgd = (#Fbkgdh + #Fbkgd1) * #Cfactor*

`Calculate the net peak counts for F

#Fnet = #Fpeak - #Fbkgd

`Calculate the average beam current during the analysis

#nAave = #nAtot / #loop

`Calculate the total count time on the peak position

*#timetot = 10 * #loop*

At this point in the macro, the net peak counts for F are converted to units of counts/second/nA, compared with intensities measured on standard reference materials for F and k-ratio is calculated. The k-ratio is input into the Geller automation software and processed with the major and minor element data for the unknown (collected previously).